

PAPER



Cite this: *Food Funct.*, 2024, **15**, 10811

Human breast milk-derived phospholipid DOPE ameliorates intestinal injury associated with NEC by inhibiting ferroptosis†

Yanjie Chen,[‡] Wenjuan Chen,[‡] Yu Dai,[‡] Xiangyun Yan, Chengyao Jiang, Fan Zhang, Min Zhang, Xiaoshan Hu, Juyi Zhao, Tingyue Wu, Shushu Li,^{*} Shuping Han^{*} and Xiaohui Chen^{*}

Neonatal necrotizing enterocolitis (NEC) is a severe inflammatory bowel disease that commonly affects premature infants. Breastfeeding has been proven to be one of the most effective methods for preventing NEC. However, the specific role of lipids, the second major nutrient category in human breast milk (HBM), in intestinal development remains unclear. Our preliminary lipidomic analysis of the HBM lipidome revealed that dioleoyl phosphatidylethanolamine (DOPE) is not only abundant but also shows high solubility in lipids, endowing it with significant biological utility. Experimental results confirmed that DOPE significantly reduces the mortality of neonatal rats, ameliorates impairment of intestinal barrier function, and alleviates the expression of intestinal inflammatory factors IL-1 β and IL-6. Furthermore, DOPE promotes the migration and proliferation of intestinal epithelial cells, thereby enhancing the integrity of the intestinal barrier function *in vitro*. The progression of NEC is linked with the onset of ferroptosis. Our cellular-level analysis of lipid peroxide and iron ion concentrations revealed that DOPE significantly reduces the indicators of ferroptosis, while also modulating the expression of pivotal ferroptosis-associated factors, including SLC7A11, GPX4, and ACSL4. Hence, this research on DOPE is expected to provide novel insights into the bioactive lipids present in HBM.

Received 14th August 2024,
Accepted 27th September 2024
DOI: 10.1039/d4fo03904a
rsc.li/food-function

1. Introduction

Necrotizing enterocolitis (NEC) is a common gastrointestinal disease in preterm infants, with its incidence and mortality inversely correlated with gestational age and birth weight.¹ According to the latest meta-analysis, the incidence of low-birth weight infants in NICUs is approximately 7%, with a mortality as high as 20%–30%.² Due to the immature gut barrier function and immune system in preterm infants, NEC is characterized by inflammatory infiltration and necrosis of the distal small intestine and the proximal colon, which can be accompanied by intestinal perforation, peritonitis, sepsis and multiple organ dysfunction syndrome in severe cases.^{3,4} Therefore, it is of great significance to seek methods for the early prevention and treatment of NEC.

Clinical studies have found that breastfeeding reduces the incidence of NEC, especially in very low or low birth weight infants.^{5,6} It is broadly acknowledged that human breast milk (HBM) guards against NEC in premature infants due to its bioactive elements.⁷ For example, lactoferrin and antimicrobial peptides are well-recognized for their ability to hinder the adherence and invasion of pathogens to intestinal cells.⁸ Additionally, human milk oligosaccharides, serving as the principal energy source for beneficial gut bacteria, play a crucial role in fostering a robust and balanced gut microbiota.⁹ However, lipids, the second major category of nutrients in HBM, have traditionally been recognized only for their role in providing nutrition and energy, and their potential effects on the intestinal health of newborns have not yet been effectively investigated.

Currently, research has predominantly centred around the fatty acids sourced from HBM owing to the fact that triglycerides constitute 98% of the lipid content in HBM.¹⁰ Nevertheless, it is crucial to recognize that despite phospholipids (PLs) comprising only 2% of the overall lipid content in HBM, they serve as essential constituents that play a vital role in delineating HBM from formula milk.¹¹ Studies have demonstrated that PLs present in HBM play a crucial role in preserving the chemical stability of fatty acids within the HBM and

Department of Pediatrics, Women's Hospital of Nanjing Medical University, Nanjing Women and Children's Healthcare Hospital, Nanjing, Jiangsu, China.
E-mail: chenxiaohui@njmu.edu.cn, shupinghan@njmu.edu.cn, lishushu@njmu.edu.cn

† Electronic supplementary information (ESI) available. See DOI: <https://doi.org/10.1039/d4fo03904a>

‡ These authors contributed equally to this work.

facilitating their digestion and absorption in the infant's gastrointestinal tract.¹² Randomized controlled trials suggest that infant formulas enriched with phospholipid-coated lipid droplets can positively influence the long-term cognitive development and Body Mass Index (BMI).^{13–15} Conversely, the exploration into the connection between the HBM-derived phospholipid and intestinal development in neonates constitutes an uncharted territory in this field. Consequently, a detailed exploration of the functions and underlying mechanisms of HBM-derived PLs within the context of NEC holds the promise of uncovering a novel and state-of-the-art strategy for the prevention and management of this condition.

In the previous breast milk lipid omics analysis, a phospholipid that is simultaneously abundant and stable in the breast milk of term and preterm infants caught our attention: PE (18:1/18:1), dioleoyl phosphatidylethanolamine (DOPE), which is composed of two identical 18:1 fatty acid chains.¹⁶ Thus, this study aims to evaluate the therapeutic potential of DOPE in both NEC cellular and animal models, while searching for the underlying mechanisms.

2. Materials and methods

2.1 Lipid screening

The lipid screening data originate from the previous lipidomic study on preterm and term-HBM conducted by our research group. These data are accessible at the following website: <https://onlinelibrary.wiley.com/doi/10.1002/mnfr.202000845>.

The product was provided by Merck Sciences (Shanghai, China) and its purity was more than 99%. The physicochemical parameters and three-dimensional spatial structure were analysed using the online platform LipidMaps (<https://www.lipidmaps.org>), which is referred to as DOPE based on its English abbreviation. We dissolved the lipid powder in a solvent mixture of CHCl₃:MeOH at a ratio of 9:1, then diluted it to an appropriate concentration with deionized water, and stored it at 4 °C.

2.2 In vitro experiments

2.2.1 Cell culture and cell modelling. The intestinal epithelioid cell 6 (IEC-6) was purchased from American Type Culture Collection (Manassas, VA, USA). IEC-6 was cultured in DMEM (Gibco, USA), supplemented with fetal bovine serum (10%, Gibco, USA) and penicillin/streptomycin (1%, Gibco, USA). IEC-6 was randomly divided into a control group (CTL) and a modeling group (LPS group). The control group was cultured with DMEM containing 10% serum, while the modeling group was cultured with DMEM containing 3% serum and lipopolysaccharides (LPS, 50 µg ml⁻¹, Sigma-Aldrich, USA) in a 5%CO₂ incubator at 37 °C. The L-α-phosphatidyl ethanolamine (DOPE, 5 µg ml⁻¹, purity ≥ 99%, CAS: 4004-05-1) was obtained from Sigma-Aldrich.

2.2.2 Cellular uptake assay. IEC-6 was treated with the FITC-labeled DOPE for 2 h and then fixed with 4% paraformaldehyde for 10 min, stained with DAPI for 15 min and observed

under a confocal fluorescence microscope (CARL ZEISS, Germany).

2.2.3 RNA isolation and quantitative real-time PCR (qRT-PCR). RNA from cells and tissues was extracted using the Freezol Regent R711-01 (Vazyme, China). The sample was placed in a freezer at -80 °C for storage until use. According to the instructions for qPCR, reverse transcription of gRNA into cDNA was performed using a cDNA synthesis kit (Vazyme, China). The mixed cDNA samples were used for PCR with SYBR Green (Servicebio, China) in a 20 mol L⁻¹ volume. PCR amplification was then performed using a Real-Time System (Applied Biosystems, USA). The sequences of primers are shown in Table 1. Data were calculated using the 2^{-ΔΔCt} method.

2.2.4 Western blot. Cell or tissue samples were mixed with RIPA buffer, protease inhibitor and phosphatase inhibitor (Beyotime, China) at a ratio of 100:1:1, and centrifuged at 12 000 rpm at 4 °C for 30 min after cracking on ice. The BCA assay kit (Thermo Fisher Scientific, USA) was used for protein quantification. The protein samples (30 µg) were isolated using SDS-PAGE and transferred to PVDF membranes (Millipore, Billerica, MA, USA). Membranes were blocked at room temperature using 5% skim milk for 2 h, incubated with the diluted primary antibody overnight at 4 °C, eluted with TBST with the residual antibody 3 times, and then incubated with the secondary antibody at room temperature for 1 h. An Immobilob™ Western Chemiraycent HRP substrate (Millipore, Billerica, MA, USA) was used to develop images of the membrane strips. Our study's primary antibodies were purchased from Protientech (China).

2.2.5 Cell proliferation and migration detection. Cell proliferation of IEC-6 was assessed using a BeyoClick™ EdU Cell Proliferation Kit (Beyotime, China). The tip of a sterile tube was used to scrape off a layer of cells in the center of a six-well plate covered with cells to form a single epithelial cell wound. DOPE was added to serum-free medium for 1 h before LPS exposure, and scratch areas were observed under the microscope for 0 and 6 hours, respectively. The cell migration area was calculated using ImageJ software.

2.2.6 Reagents related to ferroptosis. Reactive Oxygen Species (ROS) fluorescence detection, malondialdehyde (MDA)

Table 1 Primer sequences

Primer name	Sequence
Rat-GAPDH-F	AGGTCGGTGTGAACGGATTG
Rat-GAPDH-R	TGTAGACCATGTAGTTGAGGTCA
Rat-IL-1β-F	GGCTTCCTTGTGCAAGTGTC
Rat-IL-1β-R	GGCTTCCTTGTGCAAGTGTC
Rat-IL-6-F	AGAGACTTCCAGCCAGTTGC
Rat-IL-6-R	TGGTCTTGGTCCTTAGCCAC
Rat-ZO-1-F	CTGCCACACTGTGACCCT
Rat-ZO-1-R	ACAGTTGGCTCCAACAAGGT
Rat-Occludin-F	TTACGGCTACGGAGGGTACA
Rat-Occludin-R	TAGTCAGATGGGGGTGGAGG
Rat-GPX4-F	ATACGCTGAGTGTGTTTGC
Rat-GPX4-R	CTTCATCCACTTCCACAGCG

content determination, bivalent iron ion fluorescence detection (Dojindo, Japan) and GSH level detection (Wanleibio, China) in cell and animal experiments were performed according to the instructions. Ferroptosis inducer RSL3 was purchased from MedChemExpress (MCE, New Jersey, USA).

2.3 *In vivo* experiments

2.3.1 Animal models. This study was ethically reviewed and approved by the Institutional Review Board (IRB) of the Women's Hospital of Nanjing Medical University, Nanjing Women and Children's Healthcare Hospital. Neonatal SD rats were divided into 3 groups within 24 hours after birth: control group, NEC group, and NEC + DOPE group, with 12 rats in each group. Rats in the CTL group were fed by their mothers, while rats in the NEC group were given 50 $\mu\text{L g}^{-1}$ formula (Similac Advance infant formula (Abbott Nutrition): Esbilac dog milk substitute, 2 : 1) by gavage 3 times a day, stimulated with hypoxia (5% O_2 , 95% N_2) for 5 minutes prior to each gavage. In the NEC + DOPE group, DOPE (1 mg kg^{-1}) was added to the formula milk for gavage. The number of dead rats in each group was recorded daily, and the pups were killed after 4 days of modeling. The terminal ileum samples were taken, fixed with 4% paraformaldehyde and embedded with paraffin, which were used for hematoxylin–eosin staining and immunohistochemical analysis.

2.3.2 Hematoxylin–eosin staining. The paraffin-embedded terminal ileum specimen was sectioned into slices 5 microns in thickness. Following dewaxing and rehydration, the sections were stained with hematoxylin at room temperature for 30 seconds. After color separation, the sections were counterstained with eosin for 2–3 minutes. Subsequently, the sections underwent dehydration and clearing processes before being observed under a light microscope (Zeiss, Germany).

2.3.3 Immunohistochemistry. After deparaffinization, rehydration and antigen retrieval, the paraffin-embedded sections were incubated with a blocking solution of goat serum for 1 hour to prevent non-specific binding. Subsequently, an appropriate amount of the primary antibody was applied to the sections and they were stored in a wet box at 4 °C overnight. The following day, the sections were washed with PBS buffer to remove any unbound material, and then the secondary antibody was added and incubated at room temperature for 2 hours. Finally, the slides were colored with a chromogenic solution and examined under a light microscope (Zeiss, Germany).

2.3.4 Immunofluorescence staining. Prior to incubation with the primary antibody at 4 °C overnight and the secondary antibody at room temperature the following day, the paraffin sections were first sealed with a solution of 5% bovine serum albumin (BSA) for 1 hour at room temperature. Subsequently, the samples were stained with DAPI nuclear dye (Sigma Aldrich, USA) to enhance the visualization of the nucleus.

2.4 Data analysis

The analysis and statistical graph plotting were performed using GraphPad Prism 9.0 software. All experimental data were obtained from three or more independent experiments. Data that

were normally distributed were expressed as mean \pm standard deviation. The comparison between two groups was conducted using an independent sample *t*-test, while one-way analysis of variance (ANOVA) was employed for comparisons among multiple groups. A *P*-value less than 0.05 was considered statistically significant (**P* < 0.05; ***P* < 0.01; ****P* < 0.001).

3. Results

3.1 Screening and characteristics of DOPE

A total of 395 lipids were identified by our previous lipidomic analysis of HBM (Table S1†). Combined with the signal intensity of mass spectrometry, we found that phosphatidylethanolamine was abundant and ranked second after triglycerides in the variety distribution of HBM (Fig. 1A and B). The direct content analysis showed that PE (18:1/18:1) was the highest among the top three lipids (Fig. 1C). Its chemical structure formula is $\text{C}_{41}\text{H}_{78}\text{NO}_8\text{P}$, and molecular weight is 744.03 according to the Lipidmaps database. Utilizing the Chemdraw 20.0 software, we gain insight that DOPE is a phospholipid composed of two identical monounsaturated fatty acids, specifically oleic acid (C18:1) (Fig. 1D). We named it DOPE according to the English abbreviation. To detect the absorption of DOPE in intestinal epithelial cells, FITC-labeled DOPE was diluted in PBS buffer and added to IEC-6 medium, and significant fluorescence distribution in cytoplasm and nucleus was observed only 2 hours after administration (Fig. 1E).

3.2 Protective effects of DOPE on NEC animal models

Based on the NEC animal models, we added exogenous DOPE (1 mg kg^{-1}) and recorded the daily survival rate of newborn SD rats. After the neonatal SD rats were killed 4 days later, we observed that the terminal ileum of the NEC group was obviously congested and pneumatically inflected, with intestinal rupture and perforation in severe cases. In contrast, the appearance of intestinal tissue is significantly improved after DOPE intervention (Fig. 2A). We found that the mortality rate of the DOPE group was lower than that of the NEC group (Fig. 2B). According to the pathological scoring system of NEC,¹⁷ the injury score of the terminal ileum showed a significant decrease after DOPE intervention (Fig. 2C). In addition, the proliferative ability of the NEC group was weakened, and the levels of inflammatory factors (IL-1 β and IL-6) and inflammatory receptors TLR4 were significantly increased. Interestingly, exogenous DOPE significantly inhibited inflammation and relieved intestinal barrier and proliferation functions (Fig. 2D, E and F). Quantification of IHC for the proteins is shown in Fig. S1†.

These results indicate that exogenous DOPE can effectively alleviate the development of NEC at the animal level.

3.3 DOPE improves IEC-6 inflammation and barrier damage induced by LPS

We constructed an *in vivo* model of NEC with 3% DMEM involved in LPS stimulation (50 $\mu\text{g mL}^{-1}$). Previous studies have

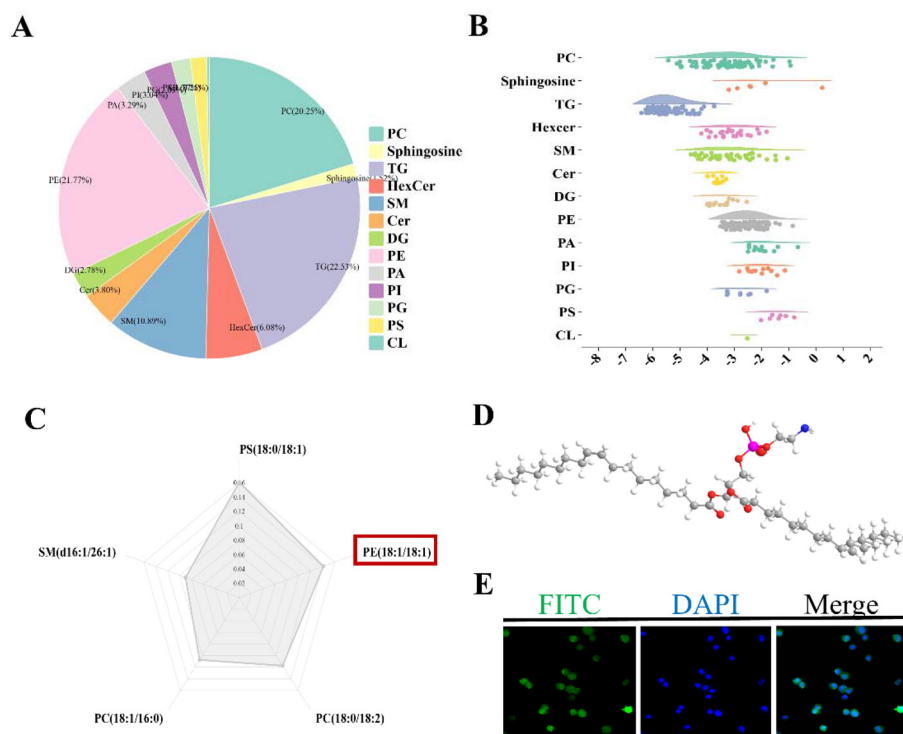


Fig. 1 Screening and characteristics of DOPE. (A) A pie chart of HBM lipid classification. (B) A cloud rain map showing the relative differences in the detected lipid contents. (C) A radar map of enriched lipids in HBM. (D) 3D molecular structure of DOPE from ChemDraw20.0. (E) Cellular internalization of DOPE in IEC-6 cells. IEC-6 was incubated with FITC-labeled DOPE (green) for 2 h and stained with DAPI (blue). Scale bar = 50 μ m, IEC6: rat small intestinal cells; FITC: fluorescein isothiocyanate; DAPI: propidium iodide; TG: triglyceride; HexCer: hexose ceramide; SM: sphingomyelin; Cer: ceramide; DG: diglyceride; PE: phosphatidyl ethanolamine; PA: phosphatidic acid; PI: phosphatidylinositol; PG: phosphoglyceride; PS: phosphatidylserine; and CL: cardiolipin.

demonstrated that the migration of epithelial cells is crucial for the repair of the intestinal barrier.¹⁸ Therefore, we investigated the effect of DOPE on the migration ability of IEC-6. The experimental results showed that the migration ability of IEC-6 was significantly inhibited under LPS stimulation, which was restored by the presence of DOPE (Fig. 3A). Through EdU proliferation experiments, it was observed that the proportion of proliferative cells in the DOPE group increased compared with that in the LPS group (Fig. 3B). The tight junction protein levels of ZO-1 and occludin (Fig. 3C and Fig. S2†) and the inflammatory cytokine levels of IL-1 β and IL-6 (Fig. 3D and E) were detected by qRT-PCR and western blot, respectively, and it showed that DOPE can reduce the expression of inflammatory cytokines and receptors and reverse the damage of barrier proteins. Consequently, it can be concluded that DOPE has the potential to alleviate the damage observed in IEC-6 cells.

3.4 Confirming the involvement of ferroptosis in NEC

Recent studies have shown that a large number of ferroptosis-related peroxidation products, such as ROS and MDA, accumulate in the damaged intestinal tissues of newborn infants with NEC.¹⁹ Therefore, an ROS fluorescent probe and an MDA assay kit were used to detect reactive oxidative stress levels in cells and animal models. As shown in Fig. 4A, in the LPS group, the

ROS fluorescence intensity of IEC-6 cells labeled with DCFH is significantly higher than that in the control group, while the levels of antioxidant glutathione peroxidase (GSH) were significantly decreased (Fig. 4B). The intervention of DOPE can significantly reverse the level of oxidative stress in IEC-6. Further to this, we conducted assessments of the cellular levels of lipid peroxidation products, specifically MDA, as well as iron concentrations. The results indicate a pronounced accumulation of both MDA and iron within the NEC group (Fig. 4C and Fig. S3†). More interestingly, DOPE was negatively correlated with the expression of the positive ferroptosis regulatory protein ACSL4, and positively correlated with the negative ferroptosis regulatory proteins SLC7A11 and GPX4 (Fig. 4D) at the molecular level. To further validate this discovery, we conducted assays to monitor the changes in ferroptosis markers at the animal level. Immunofluorescence staining and qRT-PCR analysis of terminal ileum both indicated that (Fig. 4E and F) the intervention of DOPE significantly upregulates the expression of GPX4, a key factor regulating ferroptosis in intestinal tissues. Concurrently, this intervention was observed to decrease the concentrations of MDA within the intestinal tissues (Fig. 4G). These experiments all prove that ferroptosis plays an important role in the occurrence and development of NEC.

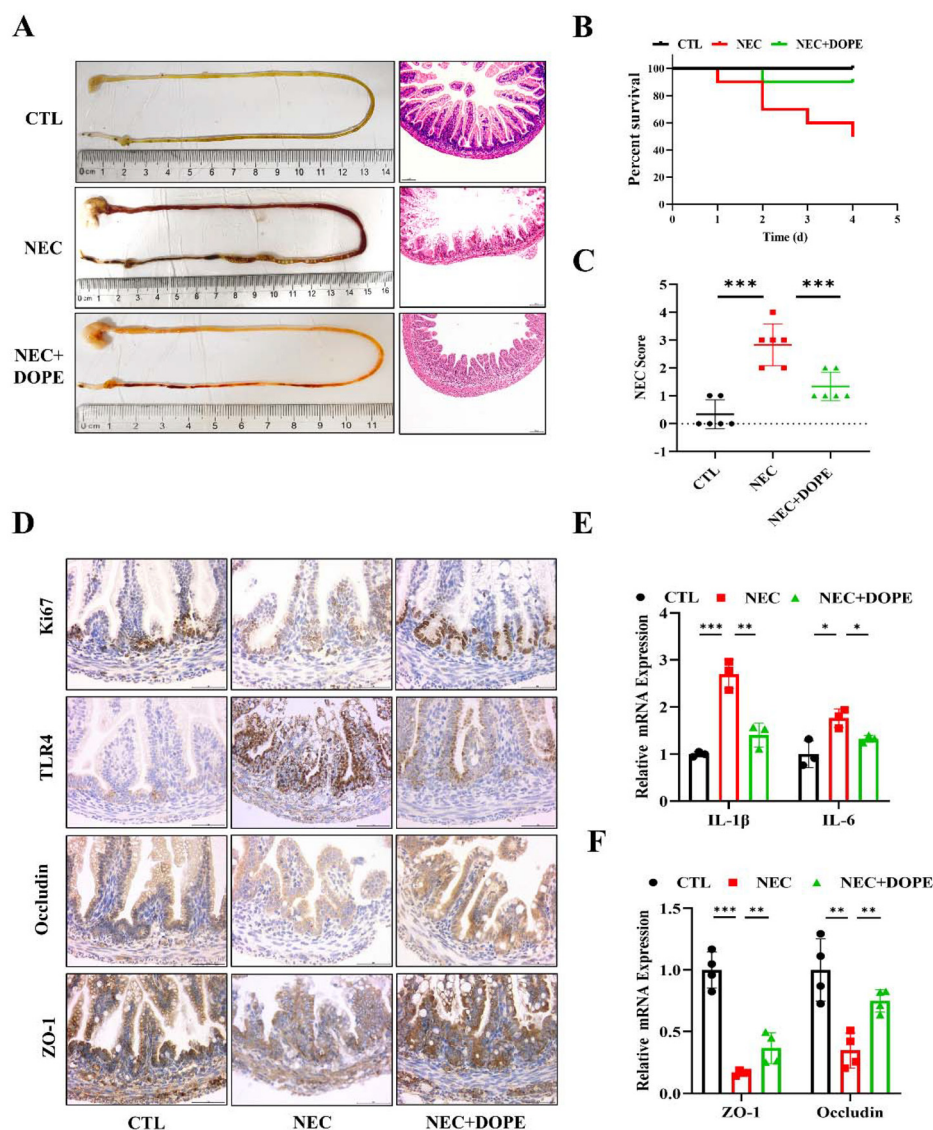


Fig. 2 Protective effect of DOPE at the *in vivo* level. (A) The terminal ileum morphology and H&E micrographs of newborn SD rats that were mother fed (CTL), exposed to experimental NEC (NEC), or administered with DOPE at 1 mg kg⁻¹ (NEC + DOPE), scale bar = 10 μm. (B) Survival rate of neonatal rats at 4 days after birth. (C) Intestinal NEC pathological score was quantified in each group. (D) Immunohistochemical imaging of TLR4, Ki67, ZO-1 and occludin in the terminal ileum, scale bar = 1 μm. (E) The transcription levels of IL-1β and IL-6 in terminal ileum. (F) The transcription levels of ZO-1 and occludin in the terminal ileum. **p* < 0.05, ***p* < 0.01, and ****P* < 0.001.

3.5 DOPE exhibits certain anti-ferroptosis properties

We induced ferroptosis in IEC-6 using a GPX4 inhibitor RSL3 (100 ng ml⁻¹) and simultaneously performed DOPE intervention. The experimental outcomes indicated that following DOPE intervention, there was a significant reduction in the number of ROS-positive cells compared to the RSL3-induced group (Fig. 5A). Additionally, the level of lipid peroxide MDA decreased (Fig. 5B), and the intracellular antioxidant GSH levels increased (Fig. 5C). The onset of ferroptosis is typically accompanied by an imbalance in the redox system. Subsequent western blot analysis demonstrated that under RSL3 induction, the expression of the ferroptosis progression marker ACSL4 was upregulated. However, after DOPE interven-

tion, the expression of protective markers GPX4 and SLA7A11 proteins improved, indicating a favourable shift in ferroptosis-related indicators when compared to the RSL3 group (Fig. 5D). These experimental findings robustly demonstrate that DOPE possesses substantial anti-ferroptosis properties.

3.6 DOPE enhances NEC intestinal epithelial cell function by inhibiting ferroptosis

To further demonstrate the relationship between the intestinal repair function of DOPE and ferroptosis pathway, we activated ferroptosis with the inducer RSL3. Exogenous addition of DOPE revealed significant improvements in intestinal epithelial cell migration (Fig. 6A), proliferation (Fig. 6B), and

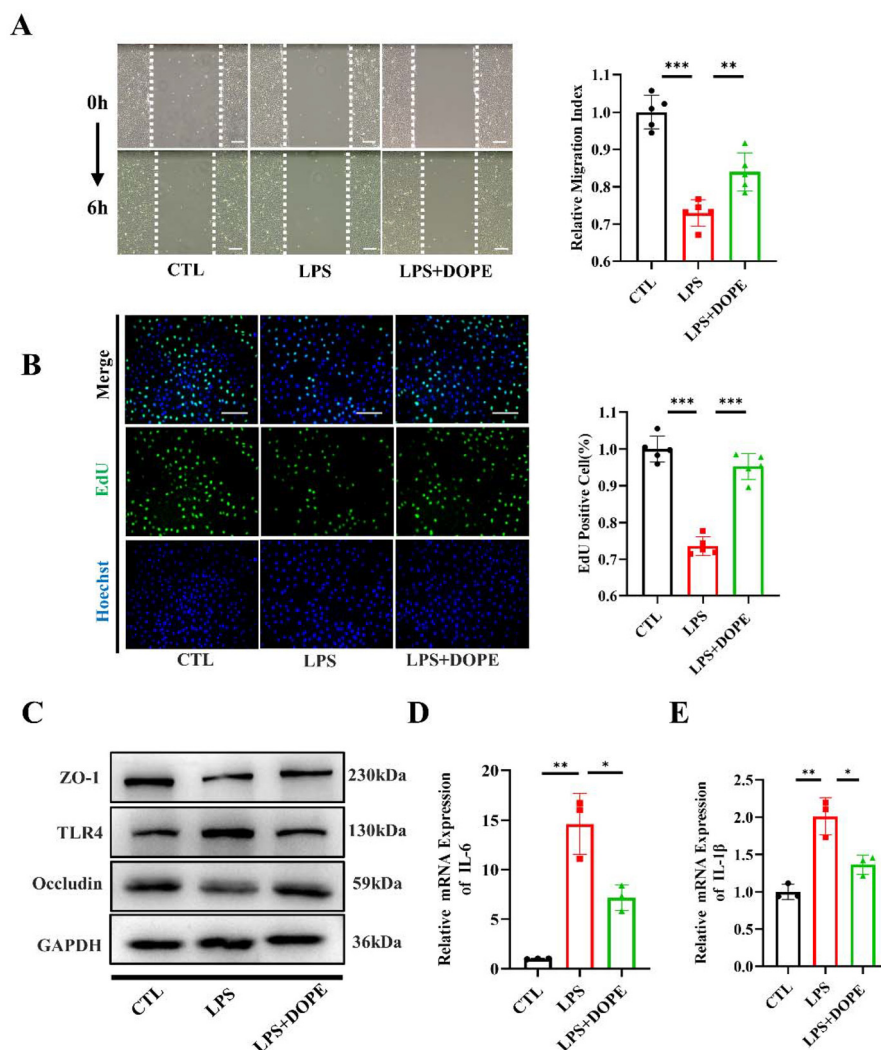


Fig. 3 Protective effect of DOPE at the *in vitro* level. (A) Cell migration was evaluated by the scratch closure test from each group, $n = 5$. Scale bar = 100 μm . (B) Cell proliferation of each group was evaluated by EDU staining, $n = 5$, scale bar = 200 μm (C) western blot showing the expression of inflammatory receptor protein TLR4 and tight junction proteins ZO-1 and occludin. (D and E) Inflammatory cytokines (IL-6 and IL-1 β) in IEC-6 were detected by qRT-PCR. $n = 3$. * $p < 0.05$, ** $p < 0.01$, and *** $p < 0.001$.

barrier function (Fig. 6C). In conclusion, DOPE improves intestinal function during NEC by inhibiting the ferroptosis signaling pathway.

4. Discussion

The lipid profiles within HBM exhibit a profound correlation with the gastrointestinal health of neonates. In this study, we innovatively found a rich bioactive lipid in HBM – dioleoyl phosphatidylethanolamine (DOPE), which is composed of glycerol, two identical monounsaturated fatty acid chains C18:1, and an ethanolamine group. Utilizing confocal microscopy, we observed that DOPE exhibits a high lipid solubility and molecular bioavailability, enabling it to freely traverse cell membranes and integrate into the epithelial cells. Furthermore, it

was observed that exogenous DOPE significantly decreased the mortality rate and severity of intestinal necrosis in neonatal SD rats, indicating that DOPE possesses a protective effect against NEC. The formation of an intact intestinal barrier is contingent upon the proliferation and migration of intestinal epithelial cells, as well as the integrity of the tight junctions that interconnect these cells.²⁰ The intervention of DOPE significantly reversed the inhibitory effects of LPS on the proliferation and migration of intestinal epithelial cells, and the expression of occludin and ZO-1 was also improved by DOPE. The functional consistency at both the cellular and animal levels demonstrates that DOPE can participate in the repair of intestinal damage.

The antioxidant defense systems in preterm infants are immature, which significantly contributes to the onset and progression of NEC by way of oxidative stress-related injury.²¹

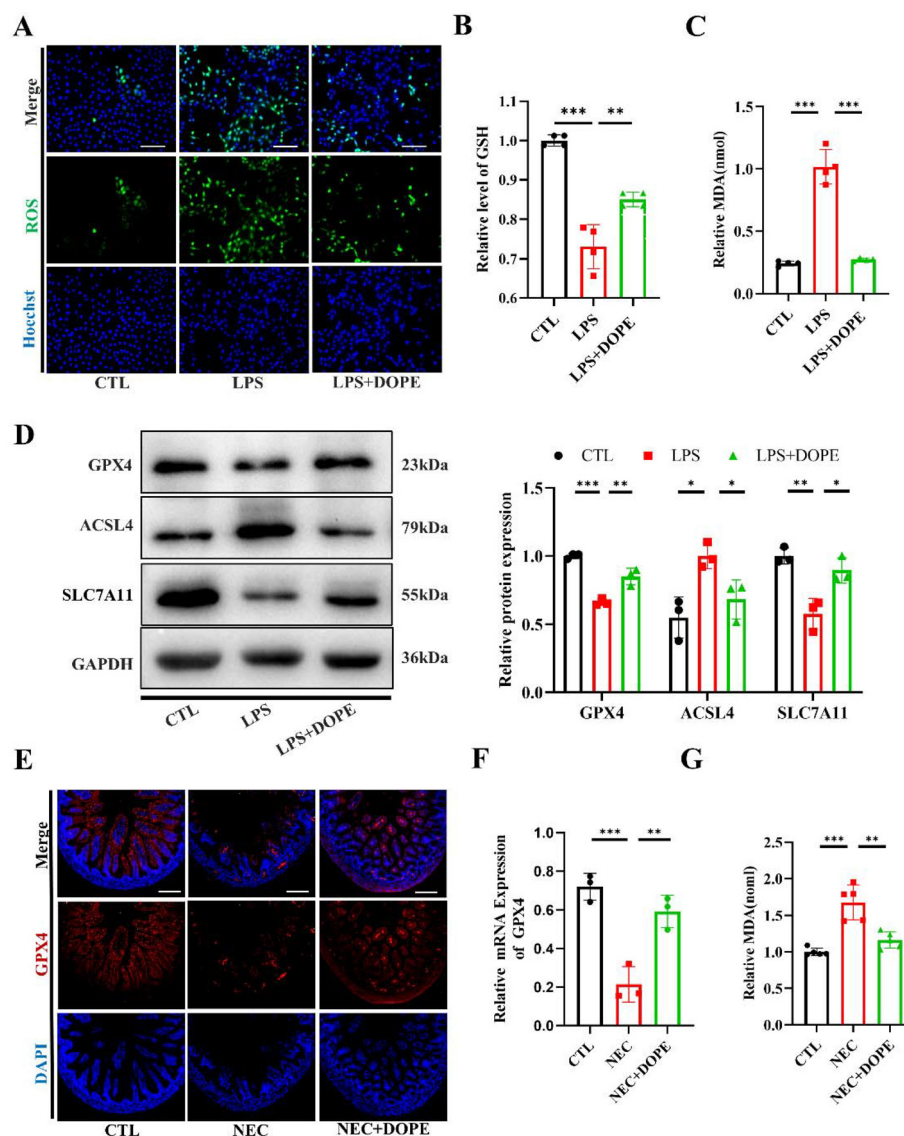


Fig. 4 The functional improvement of DOPE on IEC-6 and rat models may be related to ferroptosis. (A) ROS levels in each group at the cellular level, scale bar = 200 μ m. (B) GSH levels in each group at the cellular level. (C) MDA content in each group at the cellular level. (D) Western blot showing the expression of key proteins (SLC7A11, GPX4, and ACSL4) related to ferroptosis in IEC-6. (E) Immunofluorescence of GPX4 in the terminal ileum of neonatal SD rats, $n = 3$, scale bar = 500 μ m. (F) The transcription level of GPX4 in the terminal ileum through qRT-PCR. (G) The concentration of malondialdehyde (MDA) in the terminal ileum. $n = 3$. * $p < 0.05$, ** $p < 0.01$, *** $p < 0.001$.

Furthermore, the specific types of fats consumed in the diet are intimately associated with the inflammatory responses and the preservation of antioxidant capabilities within the gastrointestinal tract.²² Thus, this study initially assessed the changes in ROS and GSH levels before and after NEC modelling, thereby substantiating the disruption of the redox system typically observed in NEC. Lipid peroxidation products serve as valuable markers for assessing the extent of oxidative stress.²³ Recent studies have increasingly highlighted the relationship between ferroptosis and gastrointestinal diseases, including ulcerative colitis, Crohn's disease, and intestinal ischemia-reperfusion injury.^{24–26} Ferroptosis is characterized by the extensive accumulation of lipid peroxides resulting from iron ion-catalysed reactions. This

accumulation leads to an imbalance in the cellular reduction system and ultimately causes the rupture of the cell membrane.²⁷ Furthermore, the buildup of these lipid peroxides and reactive oxygen species is believed to play a crucial role in the pro-inflammatory aspects of ferroptosis.²⁸ Subsequent analysis of lipid peroxidation markers, such as MDA, and iron ion levels uncovered a remarkable insight: the onset of NEC is associated with detectable changes in ferroptosis markers. Surprisingly, intervention with DOPE was found to significantly mitigate these changes in key molecules associated with ferroptosis both in animal models and at the cellular level.

Ferroptosis is regulated by multiple metabolic pathways, including lipid, iron, and redox metabolism.²⁹ Among these,

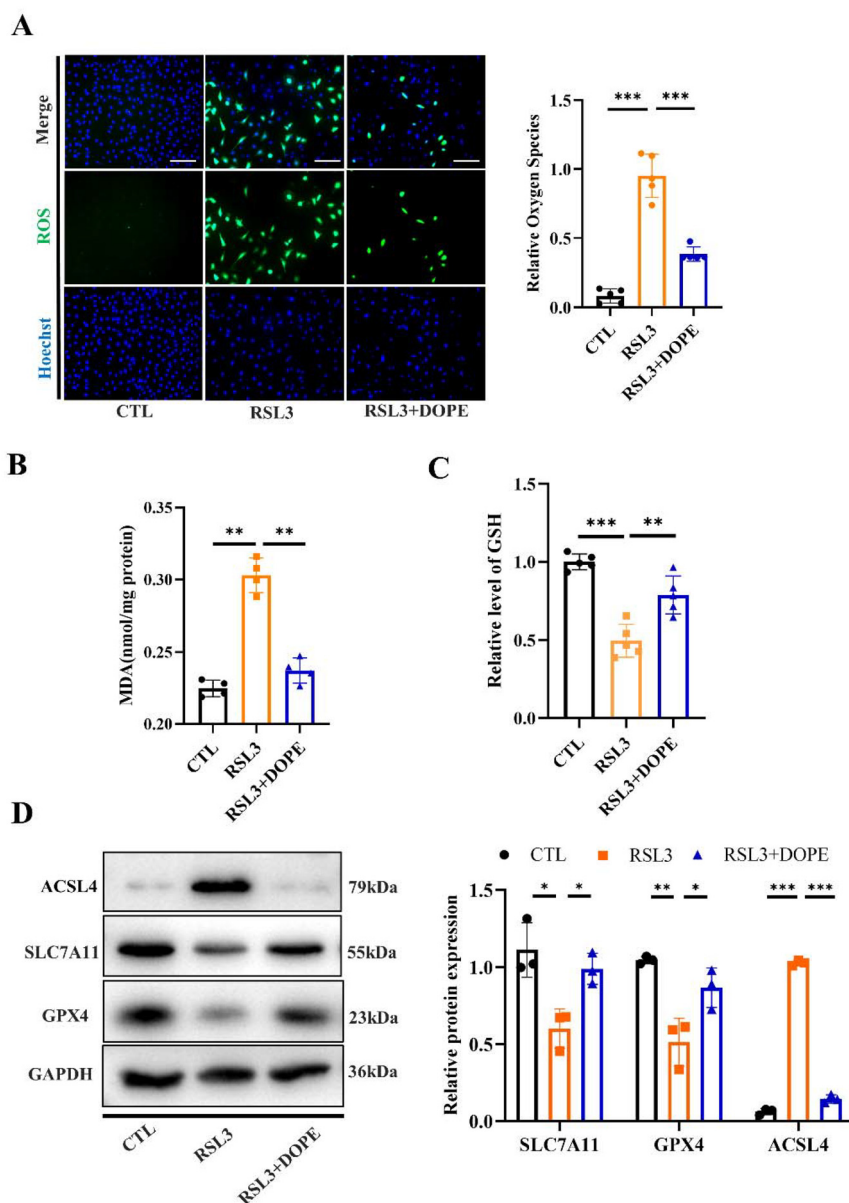


Fig. 5 DOPE suppressed ferroptosis to mediate its effect. (A) The ROS level in RSL3-induced IEC-6 treated with DOPE, scale bar = 200 μ m. (B) MDA level in each group. (C) GSH levels in each group at the cellular level. (D) Differentially expressed proteins SLC7A11, GPX4, and ACSL4 from the three groups in the ferroptosis. * $p < 0.05$, ** $p < 0.01$, *** $p < 0.001$.

the peroxidation of membrane PLs represents a critical step in the process of ferroptosis. Polyunsaturated fatty acids found in membrane PLs, particularly those containing arachidonic acid C(20:4) and adrenic acid C(22:4), play a significant role as important lipids in ferroptosis.³⁰ What exactly is the role of DOPE in ferroptosis? In order to elucidate the further mechanism of DOPE, we employed the GPX4 inhibitor, RSL3, to induce ferroptosis. With the activation of the ferroptosis signaling pathway induced by RSL3, the experimental results show that DOPE can not only regulate the expression level of key molecules of ferroptosis, but also alleviate the phenotypic damage of intestinal epithelial cells. The contemporary investigation on lipids tends to concentrate on small molecular fatty

acids and related substances, whose biological efficacy is significantly influenced by the quantity and location of double bonds.³¹ For example, it is currently acknowledged that the ratio balance of n-3/n-6 unsaturated fatty acids is closely related to lipid metabolism, anti-inflammatory and antioxidant capacity.³² Consequently, we hypothesize that the fatty acid configuration of PLs might potentially play a crucial role in their underlying mechanism.

Phosphatidylethanolamine (PE) typically constitutes a crucial component of the intestinal mucus layer. In the context of patients afflicted with inflammatory bowel disease, a notable decrease in the concentration of PE is indicative of a compromised mucus barrier, highlighting the disease's

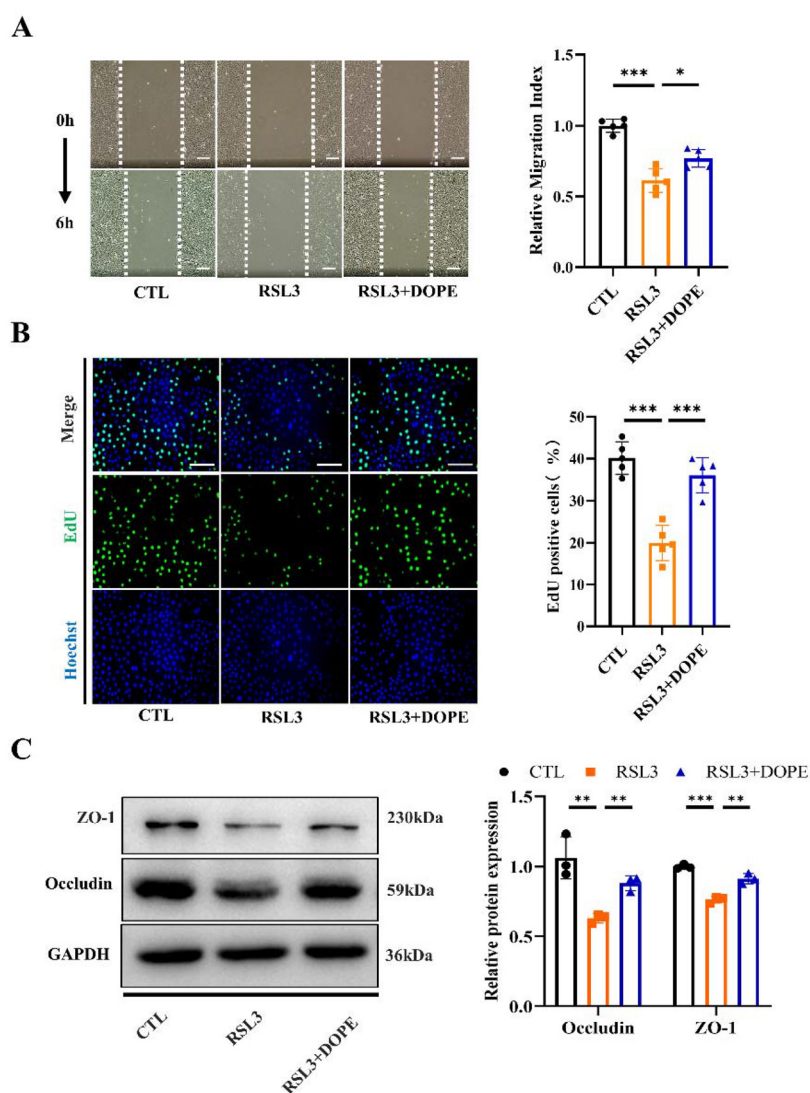


Fig. 6 DOPE suppressed ferroptosis to alleviate intestinal functional impairment. (A) Cell migration was evaluated by scratch closure test from three groups, scale bar = 100 μ m. (B) Cell proliferation of each group was evaluated by EDU staining, scale bar = 200 μ m. (C) Western Blot showing the expression of barrier associated protein (ZO-1 and occludin) in IEC-6. $n = 3$. * $p < 0.05$, ** $p < 0.01$, and *** $p < 0.001$.

impact on this protective layer.³³ The administration of formula milk enriched with PLs to preterm infants has demonstrated a reduction in the occurrence of NEC at stages II and III,³⁴ and the clinical application prospects of PLs in alleviating the condition have already emerged. Furthermore, the content of PLs is closely related to the normal functioning of biological membranes, and more than 3/4 of the lipids found in mitochondria are PLs, which display distinct distribution characteristics. Among these, PE is particularly abundant in the mitochondrial inner membrane, accounting for about 40% of all PLs.³⁵ Therefore, the homeostasis of intracellular PE is crucial for maintaining the normal metabolic activities of mitochondria. DOPE, a complex lipid composed of glycerol, phosphate, two identical monounsaturated fatty acid chains C18:1, and an ethanolamine group, is the fundamental struc-

tural component of all mammalian cell membranes and is believed to be associated with intestinal metabolic balance.³⁶ The intervention of DOPE significantly reverses the imbalance in the cellular redox system, which is in line with our experimental results. The rupture of the plasma membrane, as the ultimate outcome indicating cell ferroptosis, highlights the crucial role of DOPE in maintaining the homeostasis of the cell membrane during the occurrence of NEC.

Literature search showed that ethanolamine, the main component of DOPE, alleviates oxidative stress and maintains intestinal barrier function.³⁷ Even more impressively, its monounsaturated fatty acid chain, oleic acid (C18:1), can competitively inhibit the peroxidation process of polyunsaturated fatty acids, thus exerting anti-ferroptosis properties.³⁸ In the process of lipid peroxidation, ASCL4 preferentially selects the

free PUFA in the cell to bind to CoA for esterification, and the activated PUFA undergoes peroxidation with the PLs through LPCAT3.³⁹ Monounsaturated fatty acids (MUFAs) have been shown to competitively inhibit the incorporation of PUFAs into PLs, thereby regulating ferroptosis sensitivity by altering the balance of PUFA- and MUFA-containing PLs.⁴⁰ Therefore, the increase of exogenous DOPE may exert the properties of anti-ferroptosis by changing the content of MUFA-containing phospholipids in the membrane, thereby improving and alleviating the permeability damage of the membrane induced by NEC.

However, there are still some limitations in this study. We have verified that DOPE can negatively regulate ferroptosis-related indicators and the damage caused by ferroptosis to the intestinal epithelium at the cellular level, but there is still a lack of evidence of effective direct targeted regulation of ferroptosis by DOPE. Since the specific catabolism of DOPE *in vivo* is still unclear, we only demonstrated our scientific ideas through literature search and basic experiments, and further research on how PLs affect the plasma membrane structure (such as mitochondria) may be needed in the future. Linking specific lipids, related lipid-metabolizing enzymes, and ferroptosis pathways is critical to understanding the mechanism by which lipids shape ferroptosis sensitivity. In conclusion, DOPE in HBM may play a protective role in NEC by resisting ferroptosis. To some extent, this research may offer a novel perspective on the investigation of lipid content within HBM.

5. Conclusion

In conclusion, our investigation has preliminarily explored the impact of HBM-derived DOPE on neonatal necrotizing enterocolitis (NEC), indicating that DOPE may confer intestinal protection through a certain anti-ferroptosis effect. Given that lipids are the second most abundant nutrient category in HBM, they represent a vast and untapped resource with significant potential. The unique functions of DOPE are poised to offer valuable guidance for the innovation of HBM-based products aimed at preventing and managing NEC.

Author contributions

YJC and YD designed and carried out experiments and wrote the original draft; WJC, XYZ, YCJ, FZ, MZ, XSH, JYZ, and TYW analysed data; SSL and XHC performed writing – review, editing and supervision; SSL, XHC, and SPH performed revision of the manuscript, funding acquisition and project administration; all authors have read and agreed to the published version of the manuscript.

Data availability

The data supporting this article have been included as part of the ESI.†

Conflicts of interest

The authors declare that they have no competing interests.

Acknowledgements

This work was supported by grants from the National Natural Science Foundation of China (grant no. 82271744), the Natural Science Foundation of Jiangsu Province (BK20221182), Nanjing Medical Science and Technological Development Program (grant no. JQX23008 and YKK22149) and Jiangsu Provincial Health Commission Medical Research Project (grant no. H2023012).

References

- 1 A. Kaplina, S. Kononova, E. Zaikova, T. Pervunina, N. Petrova and S. Sitkin, Necrotizing Enterocolitis: The Role of Hypoxia, Gut Microbiome, and Microbial Metabolites, *Int. J. Mol. Sci.*, 2023, **24**, 2471.
- 2 M. Sowden, M. M. van Weissenbruch, A. N. H. Bulabula, L. van Wyk, J. Twisk and E. van Niekerk, Effect of a Multi-Strain Probiotic on the Incidence and Severity of Necrotizing Enterocolitis and Feeding Intolerances in Preterm Neonates, *Nutrients*, 2022, **14**, 3305.
- 3 A. L. Meister, K. K. Doheny and R. A. Travagli, Necrotizing enterocolitis: It's not all in the gut, *Exp. Biol. Med.*, 2020, **245**, 85–95.
- 4 J. W. Duess, M. E. Sampah, C. M. Lopez, K. Tsuboi, D. J. Scheese, C. P. Sodhi and D. J. Hackam, Necrotizing enterocolitis, gut microbes, and sepsis, *Gut Microbes*, 2023, **15**, 2221470.
- 5 F. Liu, S. P. Han, Z. B. Yu, J. Zhang, X. H. Chen, W. M. Wu, X. Chu and B. B. Liu, [Effect of breastfeeding quality improvement on breastfeeding rate in very low birth weight and extremely low birth weight infants], *Chin. J. Contemp. Pediatr.*, 2016, **18**, 937–942.
- 6 H. Xiaoshan, C. Xue, Z. Jun, L. Feng, C. Xiaohui, Y. Zhangbin and H. Shuping, Eight-year operation status and data analysis of the first human milk bank in East China, *Int. Breastfeed. J.*, 2022, **17**, 65.
- 7 K. Liu, J. Guo, J. Yang and Y. Su, The Association of Human Milk Proportion with the Clinical Outcomes of Necrotizing Enterocolitis in Preterm Infants: A Retrospective Study, *Nutrients*, 2023, **15**, 3796.
- 8 W. Chen, Y. Chen, Y. Qian, J. Zhang, X. Hu, X. Yan, C. Jiang, S. Yao, Q. Yu, X. Chen and S. Han, The casein-derived peptide YFYPEL alleviates intestinal epithelial cell dysfunction associated with NEC by regulating the PI3K/AKT signaling pathway, *Food Funct.*, 2023, **14**, 3769–3778.
- 9 M. Chichlowski, J. A. van Diepen, A. Prodan, L. Olga, K. K. Ong, G. A. M. Kortman, D. B. Dunger and G. Gross, Early development of infant gut microbiota in relation to

- breastfeeding and human milk oligosaccharides, *Front. Nutr.*, 2023, **10**, 1003032.
- 10 P. Zhao, D. Li, X. Zhang, X. Ye, Z. Zhang, Z. Liu, Z. Yan, W. Wei, Q. Jin and X. Wang, Comparison of lipid structure and composition in human or cow's milk with different fat globules by homogenization, *Food Funct.*, 2023, **14**, 5631–5643.
 - 11 Y. Liu, Y. Liu, Q. Liu, J. Zhao, W. Qiao, B. Liu, B. Yang and L. Chen, Comparison of phospholipid composition and microstructure of milk fat globules contained in human milk and infant formulae, *Food Chem.*, 2023, **415**, 135762.
 - 12 T. Wei, Y. Wu, Y. Sun, Z. Deng and J. Li, Human milk phospholipid analog improved the digestion and absorption of 1,3-dioleoyl-2-palmitoyl-glycerol, *Food Funct.*, 2023, **14**, 6106–6114.
 - 13 L. Schipper, N. Bartke, M. Marintcheva-Petrova, S. Schoen, Y. Vandenplas and A. C. S. Hokken-Koelega, Infant formula containing large, milk phospholipid-coated lipid droplets and dairy lipids affects cognitive performance at school age, *Front. Nutr.*, 2023, **10**, 1215199.
 - 14 M. Abrahamse-Berkeveld, S. N. Jespers, P. C. Khoo, V. Rigo, S. M. Peeters, R. H. van Beek, O. F. Norbruis, S. Schoen, M. Marintcheva-Petrova, E. M. van der Beek, G. M. Stoelhorst, Y. Vandenplas and A. C. Hokken-Koelega, Infant Milk Formula with Large, Milk Phospholipid-coated Lipid Droplets Enriched in Dairy Lipids Affects Body Mass Index Trajectories and Blood Pressure at School Age: Follow-up of a Randomized Controlled Trial, *Am. J. Clin. Nutr.*, 2024, **119**, 87–99.
 - 15 O. H. Teoh, T. P. Lin, M. Abrahamse-Berkeveld, A. Winokan, Y. S. Chong, F. Yap, M. Marintcheva-Petrova, E. M. van der Beek and L. P. Shek, An Infant Formula with Large, Milk Phospholipid-Coated Lipid Droplets Supports Adequate Growth and Is Well-Tolerated in Healthy, Term Asian Infants: A Randomized, Controlled Double-Blind Clinical Trial, *Nutrients*, 2022, **14**, 634.
 - 16 W. Chen, X. Chen, Y. Qian, X. Wang, Y. Zhou, X. Yan, B. Yu, S. Yao, Z. Yu, J. Zhu and S. Han, Lipidomic Profiling of Human Milk Derived Exosomes and Their Emerging Roles in the Prevention of Necrotizing Enterocolitis, *Mol. Nutr. Food Res.*, 2021, **65**, e2000845.
 - 17 M. Tuşat, R. Eroz, F. Bölükbaş, E. Özkan and H. Erdal, Evaluation of the protective and therapeutic effects of extra virgin olive oil rich in phenol in experimental model of neonatal necrotizing enterocolitis by clinical disease score, inflammation, apoptosis, and oxidative stress markers, *Pediatr. Surg. Int.*, 2024, **40**, 80.
 - 18 T. Paradis, H. Bègue, L. Basmacıyan, F. Dalle and F. Bon, Tight Junctions as a Key for Pathogens Invasion in Intestinal Epithelial Cells, *Int. J. Mol. Sci.*, 2021, **22**, 2506.
 - 19 D. Dang, C. Zhang, Z. Meng, X. Lv, Z. Li, J. Wei and H. Wu, Integrative analysis links ferroptosis to necrotizing enterocolitis and reveals the role of ACSL4 in immune disorders, *iScience*, 2022, **25**, 105406.
 - 20 W. T. Kuo, M. A. Odenwald, J. R. Turner and L. Zuo, Tight junction proteins occludin and ZO-1 as regulators of epithelial proliferation and survival, *Ann. N. Y. Acad. Sci.*, 2022, **1514**, 21–33.
 - 21 C. Lembo, G. Buonocore and S. Perrone, Oxidative Stress in Preterm Newborns, *Antioxidants*, 2021, **10**, 1672.
 - 22 T. E. Adolph, M. Meyer, J. Schwärzler, L. Mayr, F. Grabherr and H. Tilg, The metabolic nature of inflammatory bowel diseases, *Nat. Rev. Gastroenterol. Hepatol.*, 2022, **19**, 753–767.
 - 23 M. S. Mortensen, J. Ruiz and J. L. Watts, Polyunsaturated Fatty Acids Drive Lipid Peroxidation during Ferroptosis, *Cells*, 2023, **12**, 804.
 - 24 Y. Wu, L. Ran, Y. Yang, X. Gao, M. Peng, S. Liu, L. Sun, J. Wan, Y. Wang, K. Yang, M. Yin and W. Chunyu, Deferasirox alleviates DSS-induced ulcerative colitis in mice by inhibiting ferroptosis and improving intestinal microbiota, *Life Sci.*, 2023, **314**, 121312.
 - 25 Y. Gao, Z. Zhang, J. Du, X. Yang, X. Wang, K. Wen and X. Sun, Xue-Jie-San restricts ferroptosis in Crohn's disease via inhibiting FGL1/NF- κ B/STAT3 positive feedback loop, *Front. Pharmacol.*, 2023, **14**, 1148770.
 - 26 W. Cai, L. Liu, X. Shi, Y. Liu, J. Wang, X. Fang, Z. Chen, D. Ai, Y. Zhu and X. Zhang, Alox15/15-HpETE Aggravates Myocardial Ischemia-Reperfusion Injury by Promoting Cardiomyocyte Ferroptosis, *Circulation*, 2023, **147**, 1444–1460.
 - 27 J. Liu, R. Kang and D. Tang, Signaling pathways and defense mechanisms of ferroptosis, *FEBS J.*, 2022, **289**, 7038–7050.
 - 28 X. Chen, R. Kang, G. Kroemer and D. Tang, Ferroptosis in infection, inflammation, and immunity, *J. Exp. Med.*, 2021, **218**, e20210518.
 - 29 D. Tang, X. Chen, R. Kang and G. Kroemer, Ferroptosis: molecular mechanisms and health implications, *Cell Res.*, 2021, **31**, 107–125.
 - 30 L. E. Pope and S. J. Dixon, Regulation of ferroptosis by lipid metabolism, *Trends Cell Biol.*, 2023, **33**, 1077–1087.
 - 31 L. F. Stinson and A. D. George, Human Milk Lipids and Small Metabolites: Maternal and Microbial Origins, *Metabolites*, 2023, **13**, 422.
 - 32 I. Djuricic and P. C. Calder, Beneficial Outcomes of Omega-6 and Omega-3 Polyunsaturated Fatty Acids on Human Health: An Update for 2021, *Nutrients*, 2021, **13**, 2421.
 - 33 A. Thomaidou, O. Deda, O. Begou, A. Lioupi, A. Kontou, H. Gika, E. Agakidou, G. Theodoridis and K. Sarafidis, A Prospective, Case-Control Study of Serum Metabolomics in Neonates with Late-Onset Sepsis and Necrotizing Enterocolitis, *J. Clin. Med.*, 2022, **11**, 11682.
 - 34 B. N. Alshaikh, A. Reyes Loredó, M. Knauff, S. Momin and S. Moossavi, The Role of Dietary Fats in the Development and Prevention of Necrotizing Enterocolitis, *Nutrients*, 2021, **14**, 145.
 - 35 J. E. Vance, Phosphatidylserine and phosphatidylethanolamine in mammalian cells: two metabolically related aminophospholipids, *J. Lipid Res.*, 2008, **49**, 1377–1387.
 - 36 L. V. Boldyreva, M. V. Morozova, S. S. Saydakova and E. N. Kozhevnikova, Fat of the Gut: Epithelial

- Phospholipids in Inflammatory Bowel Diseases, *Int. J. Mol. Sci.*, 2021, **22**, 11682.
- 37 A. Poli, C. Agostoni and F. Visioli, Dietary Fatty Acids and Inflammation: Focus on the n-6 Series, *Int. J. Mol. Sci.*, 2023, **24**, 4567.
- 38 J. Zhou, X. Xiong, K. X. Wang, L. J. Zou, P. Ji and Y. L. Yin, Ethanolamine enhances intestinal functions by altering gut microbiome and mucosal anti-stress capacity in weaned rats, *Br. J. Nutr.*, 2018, **120**, 241–249.
- 39 J. Mann, E. Reznik, M. Santer, M. A. Fongheiser, N. Smith, T. Hirschhorn, F. Zandkarimi, R. K. Soni, A. L. Dafré, A. Miranda-Vizuete, M. Farina and B. R. Stockwell, Ferroptosis inhibition by oleic acid mitigates iron-overload-induced injury, *Cell Chem. Biol.*, 2024, **31**, 249–264.
- 40 B. Qiu, F. Zandkarimi, C. T. Bezjian, E. Reznik, R. K. Soni, W. Gu, X. Jiang and B. R. Stockwell, Phospholipids with two polyunsaturated fatty acyl tails promote ferroptosis, *Cell*, 2024, **187**, 1177–1190.